Complexation of Metal Ions in Langmuir Films Formed with Two Amphiphilic Dioxadithia Crown Ethers

Yohann Corvis,[†,#] Beata Korchowiec,[‡] Jacek Korchowiec,[§] Mounia Badis,[†] Ewa Mironiuk-Puchalska,[||] Izabela Fokt,[⊥] Waldemar Priebe,[⊥] and Ewa Rogalska*[,†]

Groupe d'Etude des Vecteurs Supramoléculaires du Médicament, Faculté des Sciences, BP 239, UMR 7565 CNRS/Nancy Université, 54506 Vandoeuvre-lès-Nancy cedex, France, Faculty of Chemistry, Department of Physical Chemistry and Electrochemistry, Jagiellonian University, ul. R. Ingardena 3, 30-060 Krakow, Poland, Faculty of Chemistry, Department of Theoretical Chemistry, Jagiellonian University, ul. R. Ingardena 3, 30-060 Krakow, Poland, Faculty of Chemistry, Warsaw University of Technology, ul. Noakowskiego 3, 00-664 Warsaw, Poland, and Department of Experimental Therapeutics, the University of Texas M. D. Anderson Cancer Center, Houston, Texas 77030

Received: April 9, 2008; Revised Manuscript Received: June 4, 2008

The two new crown ethers presented in this study were synthesized in order to investigate two important features of ionophores, namely metal cation complexation and interfacial properties, and the way in which they interrelate. The two derivatives were conceived as analogs of membrane phospholipids with respect to their amphiphilicity and geometry. They contain a hydrophilic 1,1′-dioxo-3,3′-dithio-14-crown ether headgroup and bear two myristoyl or stearoyl lateral chains. The length of the myristoyl and stearoyl derivatives in an extended conformation is comparable with the thickness of the individual leaflets of cell membranes. The membrane-related and complexation properties of the two crown ether derivatives were studied in monomolecular films spread on pure water and on aqueous solutions of mono-, di-, and trivalent metal salts. The properties of the monolayers are described quantitatively using thermodynamic models. The compression isotherms of the monolayers formed on different subphases show a clear-cut differentiation of the monovalent and di- or trivalent cations with both ligands. This differentiation was interpreted in terms of conformational changes occurring in the crown ether derivatives upon complexation. Molecular modeling indicates that the mono- and divalent cations are coordinated differently by the ligands, yielding complexes with different conformations. The differences of the conformations of the mono- and di- or trivalent cation complexes may be important from the point of view of the interactions with lipid membranes and the biological activity of these potential ionophores.

1. Introduction

Cyclic polyethers termed crown ethers were first synthesized in 1967 by Charles Pedersen.[1,2] Crown ethers are highly diversified heterocycles that, in their simplest form, are cyclic oligomers of dioxane.[3] However, other electrodonor atoms such as nitrogen and sulfur often replace oxygen. Due to the host−guest complexation and molecular recognition properties, crown ethers proved useful in sensing,[4] switching,[5] phase transfer catalysis,[6] extraction,[7] and chromatography.[8,9] Crown ethers were used as well as membrane forming amphiphiles,[10] and biomimetic receptors[11] and, due to their ionophoretic properties, as model ion channels.[12]

The selective receptor properties of crown ethers together with the relative ease of preparation of a broad range of derivatives make these molecules attractive targets as ionophores. Several crown ether ionophores binding in 1:1 or 2:1 ligand:metal cation complexes were reported in the literature.[3] The ability to complex cations, which is among the most important properties of crown ethers, has been extensively studied.[13−16] The selectivity of complexation was often interpreted in terms of the size of the crown ether's cavity and the size of the cations. It is reasonable to assume that binding will be optimal when the crown ether's interior cavity is about the same size as a given cation. However, the concept of size similarity cannot be used as a unique and general explanation of molecular recognition,[17] and different aspects of metal cation complexation in these systems remain to be clarified.

Amphiphilicity is one more important property of crown ether derivatives. It was shown that various amphiphilic single-, two- and three-armed diazacrown derivatives[18] form different types of aggregates in an aqueous environment.[19−22] It was shown as well that two crowns connected by a hydrocarbon chain, the so-called bola-amphiphiles, may form stable vesicles[10] and micelles.[23,24] On the other hand, the amphiphilicity of crown ethers allowed insertion of these molecules into lipid membranes.

The complexation and membrane-related characteristics of crown ether derivatives can be studied simultaneously using the Langmuir film technique.[25−30] Indeed, it was shown that complexation of metal ions by the crown ether monolayer formed at the air−water interface affects the monolayer properties and can be correlated with the macrocycle-cation selectivity.[31−33] Moreover, the Langmuir film technique allows study of the behavior of amphiphilic macrocycles in a lipid environ-

* Corresponding author. E-mail: rogalska@lesoc.uhp-nancy.fr. Telephone: +33 (0)3 83 68 43 45. Fax: +33 (0)3 83 68 43 22.
[†] Nancy Université.
[‡] Department of Physical Chemistry and Electrochemistry, Jagiellonian University.
[§] Department of Theoretical Chemistry, Jagiellonian University.
[||] Warsaw University of Technology.
[⊥] The University of Texas M. D. Anderson Cancer Center.
[#] Present address: Laboratoire de Chimie Physique, Faculté de Pharmacie, Université Paris Descartes, 4 Avenue de l'Observatoire, 75006 Paris, France.

10.1021/jp803072b CCC: $40.75
Published on Web 08/12/2008

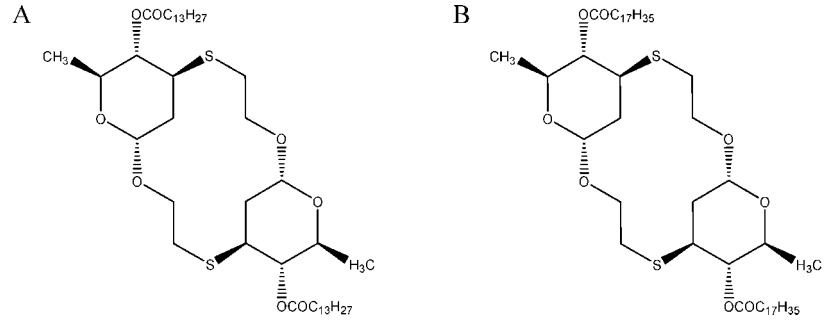

Figure 1. Structures of the amphiphile dioxadithia crown ethers studied in this work. (A) **CE1** and (B) **CE2**.

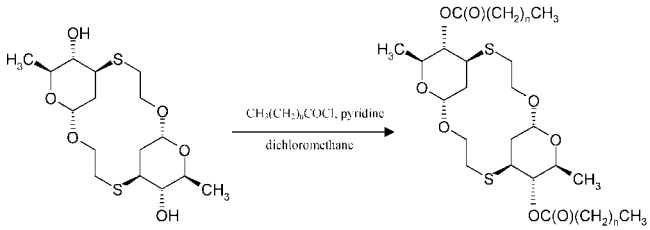

Figure 2. Synthesis of the hexopyranose-based dioxadithia crown ethers **CE1** and **CE2**.

ment.[34] Recently, the role of azacrown ether in Cu^{2+} ion recognition was investigated at the air−water interface using the Langmuir technique.[25] Importantly, the amphiphilicity of crown ethers can be adjusted by grafting lateral chains of different lengths to the crown. This is particularly easy in the case of the azacrown ethers, which can be readily substituted at the nitrogen atoms.[3,35]

The amphiphilic and complexation properties of crown ether derivatives make them particularly interesting as model membrane channels.[36−39] The synthetic channels developed by Gokel et al.[40] called hydraphiles, consist of two headgroup crown ethers connected to a hydrophobic spacer chain that is, in turn, linked to a central crown ether.[41,42] The overall length of the compound is about 42 Å, which is the approximate distance needed to span the membrane hydrocarbon core. Hydraphile channels have demonstrated activity in phospholipid vesicles[41,43] and biological systems.[44] It is known that the form[45,46] and the conformation[47] of membrane channels are essential for the transport mechanism; the synthetic models proved useful in providing structural and functional insights into ion transport across membranes. The information obtained is valuable, as no universal answer to the question of the biologically active conformation of membrane channels can be given to date, in spite of the fact that both direct physical measurements[47] and molecular dynamics simulations were used to study channel conformational rearrangements and interactions with lipid bilayers.[48−50] In the case of the dissolved Na,K ATPase a possible structural role for phospholipid stabilization of a K^+-bound conformation and preservation of enzyme activity was suggested.[51] Studies of the properties of a gramicidin/membrane system subject to external electric fields showed that the pore formation time depends on the interactions with the phospholipid.[49] However, the conformational preference of gramicidin A is strongly dependent on the specific environmental conditions such as the fatty acid chain length and even on the bilayer preparation method.[52] On the other hand, studies on voltage-gated potassium channels[50] showed that the presence of the channel significantly perturbs the local organization of the lipid bilayer. Indeed, the bilayer is compressed in the immediate vicinity of the channel, resulting in lipid tail interdigitation and coiling around the hydrophobic surface of the channel. Taking into account the complexity of biological systems, synthetic ionophores are attractive tools for studies of channel−membrane interactions.

Two new crown ethers used in the present study were synthesized with the aim of deepening the understanding of two important features of ionophores, namely metal cation complexation and interfacial properties, and their interrelationship. The two derivatives were conceived as analogs of membrane phospholipids from the point of view of their amphiphilicity and geometry. The molecules used contain a hydrophilic 1,1′-dioxo-3,3′-dithio-14-crown ether headgroup and bear two myristoyl or stearoyl lateral chains (Figure 1). The length of the myristoyl and stearoyl derivatives in an extended conformation is, respectively, around 21 and 26 Å, which compares well with the thickness of the lipid membrane leaflets.

The properties of the new dioxadithia crown ethers were studied in monomolecular films spread at the air-aqueous interface, using the Langmuir technique. This approach allows formation of amphiphilic monolayers mimicking the individual leaflets of a membrane bilayer. The monolayers were formed on a pure water subphase, and on 0.1 M solutions of mono-, di- and trivalent metal chlorides: LiCl, NaCl, KCl, $CaCl_2$, $CdCl_2$, $CoCl_2$, $MgCl_2$, $ZnCl_2$, and $FeCl_3$. The compression isotherms were also determined as a function of salt concentration, using aqueous solutions of LiCl in the range 10^{-3} to 2 M. The compression experiments performed using the crown ether films spread on pure water and on a 10^{-1} M LiCl subphase as a function of temperature provide access to a thermodynamic analysis of the properties of the monolayers. On the other hand, molecular modeling of free ligands and metal cation complexes allowed a reliable interpretation of the experimental results in terms of conformational rearrangements of these molecules upon complexation. The overall results may be useful in the design of new synthetic membrane channels and to aid the understanding of how the channels interact with their host membranes.

2. Experimental Section

2.1. Synthesis of Crown Ethers CE1 and CE2. CE (laboratory code WP917; 100 mg, 0.24 mmol) was dissolved in dichloromethane (1 mL) and pyridine (1 mL). Mirystoyl or stearoyl chloride (266.5 mg, 1.08 mmol or 320 mg, 1.08 mmol, respectively) was added to the solution and the reaction mixture was maintained, after stirring, at room temperature. The progress of the reaction was monitored using thin layer chromatography. After the reaction was completed, the reaction mixture was diluted with dichloromethane (50 mL), washed with water (3 × 20 mL) and then with brine. The organic solution was dried over anhydrous sodium sulfate; subsequently, the drying agent was filtered off and the solvent was evaporated to dryness under

reduced pressure. The product was purified by column chromatography (silica gel 60) using hexane, then hexane: ethyl acetate 9:1 and 6:1 (v/v) as eluents. Fractions containing the desired product were combined and evaporated to dryness to give 146.1 mg of pure **CE1** (laboratory code WP1432; yield 76%) or 175.4 mg of pure **CE2** (laboratory code WP1431; yield 80%). **CE1** and **CE2** are wax-like products.

Characterization. ^{1}H NMR spectra were recorded on a Bruker AVANCE DRX 300 (300 MHz; $CDCl_3$, TMS as internal standard, chemical shifts in ppm). Mass spectra (electrospray, ES) were recorded on a Micromass Quattro Micro mass spectrometer (Waters Corporation, Milford, MA). Optical data were obtained at 20 °C on Perkin-Elmer Polarimeter 341.

CE1. ^{1}H NMR ($CDCl_3$, δ): ppm 4.79 (d, 1H, $J = 2.0$ Hz, H-1), 4.61 (dd, 1H, $J = 11.2$ Hz, $J = 9.4$ Hz, H-4), 4.05 (ddd, 1H, $J = 9.3$ Hz, $J = J = 3.5$ Hz, CH_2O linker), 3.82 (dq, 1H, $J = 9.5$ Hz, $J = 6.2$ Hz, H-5), 3.68 (ddd, 1H, $J = J = 12.9$ Hz, $J = 3.9$ Hz, H-3), 3.53 (ddd, 1H, $J = 9.3$ Hz, $J = 12.0$ Hz, $J = 3.7$ Hz, CH_2O linker), 2.82 −2.70 (m, 2H, CH_2S linker), 2.46 (dd, 1H, $J = 13.0$ Hz, $J = 3.0$ Hz, H-2e), 2.37 (dd, 2H, $J = J = 7.3$ Hz, CH_2CO), 2.89 (dd, 2H, $J = J = 6.5$ Hz, CH_2CO), 1.89 (ddd, 1H, $J = J = 13.2$ Hz, $J = 3.1$ Hz, H-2a), 1.69 (q, 2H, $J = 7.4$ Hz, CH_2 ester), 1.25 (bs, 22H, CH_2 ester), 1.16 (d, 1H, $J = 6.2$ Hz, H-6), 0.88 (t, 3H, $J = 7.0$ Hz, CH_3 ester). MS: *m/e* 801.2. $[\alpha]_D^{20} = -128°$ ($c = 2.696$, chloroform).

CE2. ^{1}H NMR ($CDCl_3$, δ): ppm 4.78 (d, 1H, $J = 2.0$ Hz, H-1), 4.60 (dd, 1H, $J = 11.2$ Hz, $J = 9.5$ Hz, H-4), 4.05 (ddd, 1H, $J = 9.3$ Hz, $J = J = 3.5$ Hz, CH_2O linker), 3.81 (dq, 1H, $J = 9.4$ Hz, $J = 6.1$ Hz, H-5), 3.68 (ddd, 1H, $J = J = 12.9$ Hz, $J = 3.9$ Hz, H-3), 3.53 (ddd, 1H, $J = 9.3$ Hz, $J = 8.1$ Hz, $J = 3.7$ Hz, CH_2O linker), 2.82 −2.70 (m, 2H, CH_2S linker), 2.46 (dd, 1H, $J = 13.2$ Hz, $J = 3.2$ Hz, H-2e), 2.3 (dd, 2H, $J = J = 6.5$ Hz, CH_2CO), 2.34 (dd, 2H, $J = J = 6.5$ Hz, CH_2CO), 1.82 (ddd, 1H, $J = J = 12.2$ Hz, $J = 3.1$ Hz, H-2a), 1.69 (q, 2H, $J = 7.0$ Hz, CH_2 ester), 1.25 (bs, 30H, CH_2 ester), 1.16 (d, 1H, $J = 6.2$ Hz, H-6), 0.88 (t, 3H, $J = 7.0$ Hz, CH_3 ester). MS: *m/e* 913.4. $[\alpha]_D^{20} = -90°$ ($c = 4.86$, chloroform).

2.2. Monolayer Experiments. Monolayer experiments were carried out with a KSV 5000 Langmuir balance (KSV, Helsinki). A Teflon trough (15 cm × 58 cm × 1 cm) with two hydrophilic Delrin barriers (symmetric compression) was used in all experiments. The system was equipped with an electrobalance and a platinum Wilhelmy plate (perimeter 39.24 mm) as a surface pressure (Π) sensor. The apparatus was closed in a Plexiglas box, and temperature was kept constant. Before each use, the trough and the barriers were cleaned using cotton soaked in chloroform, gently brushed with ethanol and then with tap water and finally rinsed with Milli-Q water (Millipore Milli-Q system, 18 MΩ cm). Milli-Q water, surface tension (γ) of 72.75 mN/m at 20 °C, was used for preparing aqueous subphases for monolayer experiments. All solvents used for cleaning the trough and the barriers, as well as products used to prepare the subphase solutions were of analytical grade. Any residual surface-active impurities were removed before each experiment by sweeping and suction of the surface. Monolayers were spread, using calibrated solutions of the crown ether derivatives of a concentration of about 1 mg/ml, prepared with spectrophotometric grade chloroform (Aldrich, ACS). After the equilibration time of 10 min, the films were compressed at the rate of 2.5 mm min^{-1} barrier^{-1} (750 mm^2 min^{-1}). A PC computer and KSV software were used to control the experiments. The standard deviation obtained from compression isotherms repeated systematically at least 3 times for each system studied was ± 0.5 Å^2 on molecular area (A) and ± 0.2 mN m^{-1} on surface pressure. Analytical grade LiCl, NaCl, KCl, $CaCl_2 \times 2H_2O$, $CdCl_2$, $CoCl_2$, $MgCl_2$, $ZnCl_2$, and $FeCl_3$ were from Sigma-Aldrich.

2.3. Computation Details. All calculations were performed at Hartree−Fock (HF) level of theory with 6−31G basis set[53,54] using GAMESS[55,56] and Gaussian[57] program packages, respectively. The geometrical structure of the ether derivatives and their complexes with Li^+, Na^+, K^+, Mg^{2+}, Ca^{2+}, and Zn^{2+} were optimized with the assumed C_2 symmetry. The closed shell complex with Cd^{2+} was not considered, because the 6−31G basis set is not available for the latter cation; the use of a different basis set for Cd^{2+} could yield the interaction energy values, which would not be directly comparable to the other cation energies. On the other hand, the open shell ions, Fe^{3+} and Co^{2+}, were excluded from calculations because the self-consistent field (SCF) process is not converged in this case. Both $-OCOC_nH_{2n+1}$ ($n = 13$ and 17) substituents were considered in the calculations. While a zigzag-type conformation of the hydrocarbon chains was assumed, the existence of other minima on the energy hypersurface can be expected due to the rotational freedom in the chains.

3. Results and Discussion

3.1. Properties of the Langmuir Films Formed with the Derivatives CE1 and CE2. The structures of the novel class of hexopyranose-based macrocycles used in this study are shown in Figures 1 and 3. These amphiphilic molecules form stable insoluble monolayers on the pure water and on various aqueous salt solution subphases. The behavior of these macrocycles in the monolayers was studied using surface pressure−molecular area (Π−A) isotherms.

The two molecules differ in their interfacial behavior, as indicated by the characteristic parameters of the compression isotherms obtained with films spread on the pure water and on the subphases containing KCl, NaCl, LiCl, $CaCl_2$, $MgCl_2$, $CdCl_2$, $CoCl_2$, $ZnCl_2$, or $FeCl_3$. The proposed orientation of these molecules at the air/water interface is presented in Figure 3. Both molecules behave differently in the presence of the salts in the subphase compared to pure water, indicating formation of crown ether−metal complexes.

3.1.1. Compression Experiments Performed at Different Concentrations of LiCl. The compression experiments performed with monolayers formed with **CE1** and **CE2** on the subphases containing different concentrations of LiCl yielded isotherms shown in Figure 4. The characteristic parameters of these isotherms[58] are collected in Table 1. It can be seen that the isotherms shift to higher molecular areas with increasing salt concentration. This result indicates that both derivatives form complexes with Li^+. The shift is observed between the concentrations 10^{-3}−10^{-1} M and 10^{-3}−10^{-2} M LiCl with **CE1** and **CE2,** respectively. For this reason, in the further experiments, the concentration of LiCl and other salts in the subphases was 10^{-1} M. It can be observed that the surface pressure at the collapse (Π_{coll}) of the monolayers formed with both derivatives increases with the concentration of LiCl in the subphase; the monolayer compressibility decreases with the LiCl concentration in the case of **CE1**, while it increases in the case of **CE2**. The latter changes, while small, indicate that the complex formed by **CE2** with Li^+ is more difficult to organize in the film compared to the complex formed by **CE1**.

3.1.2. Compression Experiments Performed with Subphases Containing Different Metal Cations. The Π−A isotherms obtained with the monolayers formed with **CE1** and **CE2** on the pure water and on the subphases containing different cations

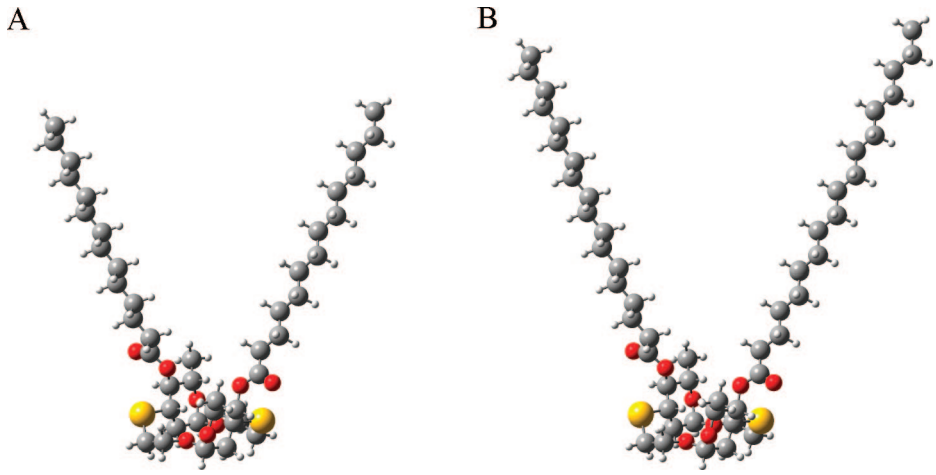

Figure 3. Proposed orientation of the **CE1** (A) and **CE2** (B) derivatives at the air/water interface. Conformations of the molecules were optimized in vacuum at the HF/6−31G level of theory.

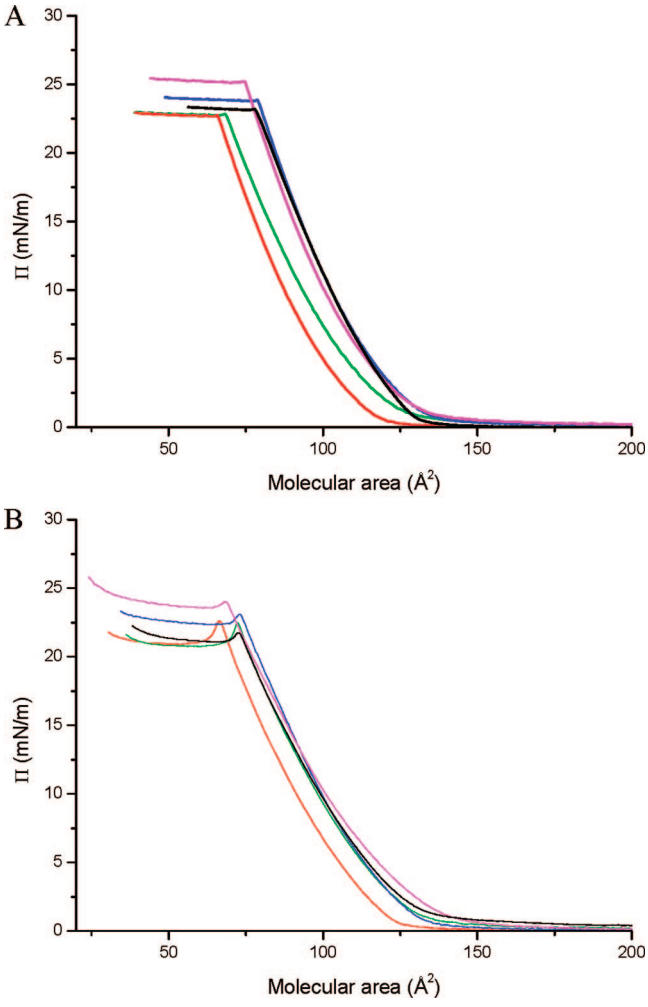

Figure 4. Π−*A* isotherms of the films formed with (A) **CE1** and (B) **CE2** on LiCl solutions. Concentration: (red line) 10^{-3} M, (green line) 10^{-2} M, (black line) 10^{-1} M, (blue line) 1 M, (magenta line) 2 M. Temperature: 20 °C.

(salt concentration 0.1 M) are shown in Figure 5. With both derivatives, the collapse pressure (Π_{coll}) values are the highest in the case of the pure water subphase (Table 2). With **CE1**, Π_{coll} rises slightly above 23 mN m^{-1} in the case of the pure water and the LiCl or $CdCl_2$ solution subphases, and is close to 22 mN m^{-1} with the other salt solution subphases. With **CE2**, the Π_{coll} values are 0.2−3.0 mN m^{-1} lower compared to the

TABLE 1: Characteristic Parameters of the Compression Isotherms Obtained with CE1 and CE2 at Different Concentrations of LiCl in the Subphase

LiCl concn [M]	$C_s^{-1}(A_0)$ [mN m^{-1}]	A_0 [Å^2]	A_{coll} [Å^2]	Π_{coll} [mN m^{-1}]	$C_s^{-1}(A_{coll})$ [mN m^{-1}]
		CE1			
10^{-3}	67.0	100	66	22.8	44.1
10^{-2}	62.3	108	68	22.8	39.4
10^{-1}	67.4	119	78	23.2	44.1
1	74.7	116	79	23.9	50.8
2	76.1	112	75	25.2	50.9
		CE2			
10^{-3}	64.6	103	67	22.6	41.9
10^{-2}	66.1	110	73	22.2	43.9
10^{-1}	57.7	117	72	21.7	35.8
1	60.7	118	74	23.0	37.8
2	55.2	121	69	24.0	31.3

films formed with **CE1**. Interestingly, the least compressible films are formed on the pure water subphase and on the subphases containing the monovalent cations in the case of **CE1** and with **CE2**, respectively.

With both derivatives, a significant shift to high molecular areas of the isotherms corresponding to the monovalent cation subphase is observed compared to pure water. In contrast, most of the isotherms obtained with di- or trivalent cation subphases are shifted toward low molecular areas in their most condensed parts compared to pure water. The effects observed indicate differences in the interactions between the crown ether derivatives and the monovalent versus di- and trivalent cations, and suggest a selective complexation.

To understand better the mechanism of the crown ether−cation complexation, thermodynamic analysis of monolayer properties and molecular modeling of the free ligands and the complexes were performed.

3.1.3. Thermodynamic Properties of Chosen Monolayers. The changes of the monolayer properties induced by cation complexation were quantified using thermodynamics. To this end, the monolayers formed with **CE1** and **CE2** were studied as a function of temperature with two different, arbitrarily chosen subphases, namely pure water and 10^{-1} M LiCl solution.

The compression isotherms obtained are shown in Figure 6 and Figure 7, and their characteristic parameters are given in Table 3 and Table 4, respectively. With both derivatives and both subphases, the values of the limiting molecular areas (A_0), as well as the molecular area taken at the collapse (A_{coll})

TABLE 2: Characteristic Parameters of the Compression Isotherms Obtained with Different Subphases

subphase[a]	$C_s^{-1}(A_0)$ [mN m^{-1}]	A_0 [Å^2]	A_{coll} [Å^2]	Π_{coll} [mN m^{-1}]	$C_s^{-1}(A_{coll})$ [mN m^{-1}]
			CE1		
water	57.0	92	54	23.5	33.5
NaCl	67.3	117	78	22.5	44.7
LiCl	67.4	119	78	23.2	44.1
KCl	66.4	116	76	22.3	44.0
$CdCl_2$	56.9	91	54	23.3	33.5
$CoCl_2$	52.5	96	55	22.1	30.2
$ZnCl_2$	54.4	92	54	22.0	32.2
$MgCl_2$	50.9	92	52	21.9	28.8
$CaCl_2$	65.9	92	60	22.5	43.4
$FeCl_3$	46.0	90	47	21.8	24.1
			CE2		
water	67.1	94	60	23.0	43.1
NaCl	54.9	123	74	21.6	33.2
LiCl	57.7	117	72	21.7	35.8
KCl	60.1	112	72	21.2	38.8
$CdCl_2$	56.9	97	62	20.3	36.5
$CoCl_2$	62.3	97	65	20.3	41.8
$ZnCl_2$	53.9	97	63	19.0	34.8
$MgCl_2$	54.1	95	57	21.7	32.4
$CaCl_2$	52.4	102	62	20.2	32.0
$FeCl_3$	56.9	93	58	21.0	35.7

[a] Salt concentration 0.1 M.

of the monolayers increase significantly between 20 and 60 °C, while the stability of the monolayers decreases slightly with temperature, as shown in the decreasing values of Π_{coll}. The increasing values of the compressibility modulus (C_S^{-1}; $C_S^{-1} = -A(\partial\Pi/\partial A)_T$)[58,59] show that all films become less compressible (more rigid) with the increasing temperature. These results suggest that the increase in thermal energy induces ordering of the molecules in the film.

The results obtained in the compression experiments at different temperatures (Tables 3 and 4) allowed calculation of the work (ΔG) needed to form monolayers on the pure water and 10^{-1} M LiCl subphases (Table 5). With both derivatives more work is required to form films on the LiCl subphase compared to pure water. However, differences were revealed between the two derivatives. Indeed, on the pure water subphase, less work is needed to form the films with the **CE1** ligand compared to **CE2**, while an opposite situation is observed with the 10^{-1} M LiCl subphase. The latter results may be linked to the less bulky structures of **CE1** and **CE2** in the case of the pure water and of the LiCl subphase, respectively, as reflected in the corresponding A_{coll} values (Table 3 and 4). It has to be noticed that for a given subphase less work is required to form films with lower C_s^{-1} values, which means that they have a more liquid-like character (Table 3 and 4).

The low, positive enthalpy (ΔH) value (63 J mol^{-1}) corresponding to the pure water subphase (Table 5) shows that the interactions between the **CE1** molecules forming the film are very weak and that the process of film formation is nearly athermal. The positive value of ΔH measured with the 10^{-1} M LiCl subphase (1100 kJ mol^{-1}) shows that the interactions between the complexed **CE1** molecules are repulsive. In the case of **CE2**, negative enthalpies are observed with both subphases; the negative heat effect (−11200 and −4600 J mol^{-1} with pure water and LiCl, respectively) can be attributed to the van der Waals interactions between the long hydrocarbon chains. Such interactions would be less important in the **CE1** molecules, bearing medium-length chains. It can be noticed that in the case of **CE2**, the enthalpy of film formation is less negative in the

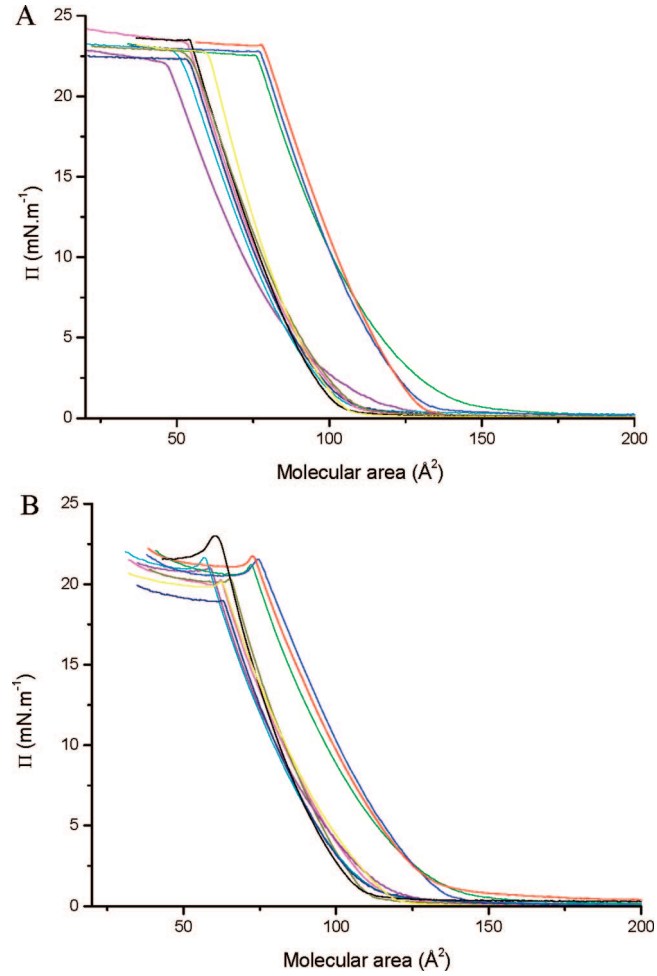

Figure 5. $\Pi-A$ isotherms of the films formed with the derivatives **CE1** (A) and **CE2** (B) on (black line) water, (red line) LiCl, (green line) KCl, (blue line) NaCl, (aqua line) $MgCl_2$, (yellow line) $CaCl_2$, (magenta line) $CdCl_2$, (orange line) $CoCl_2$, (brown line) $ZnCl_2$, and (violet line) $FeCl_3$ solutions at 20 °C. The salt concentration in the subphase was 0.1 M.

presence of LiCl compared to pure water. This effect may be responsible for the more liquid-like character of the **CE2** film formed on the LiCl compared to the pure water subphase. Overall, the enthalpy results indicate that complexation of the lithium cation may induce repulsive interactions for both derivatives. This effect may account for the observed shift of the isotherms obtained on the LiCl subphase to higher molecular areas, compared to pure water (Figure 5, Table 2).

As indicated by the entropy (ΔS) values, the ordering of the **CE2** molecules bearing the long hydrocarbon chains in the monolayers is more significant, compared to the medium-chain **CE1** molecules (Table 5). This result may account for the smaller shift between pure water and the LiCl subphase observed with **CE2**, compared to the **CE1** isotherm (Figure 5, Table 2). It was shown recently that alkyl chains may act as entropy reservoirs.[60,61] Indeed, the liberation or suppression of different modes of motion of the -CH_2 groups increases or decreases, respectively, the disorder, i.e. entropy; this controls the thermodynamic stability of the molecular organization. We propose that the long lateral alkyl chains in **CE2** play such a role upon film compression. The film compression induces ordering of the alkyl chains and a progressive loss of the motion modes. This process results in the lowering of the entropy and enthalpy of the film. Importantly, the ordering of **CE2** is more difficult in the presence of LiCl compared to pure water, as indicated

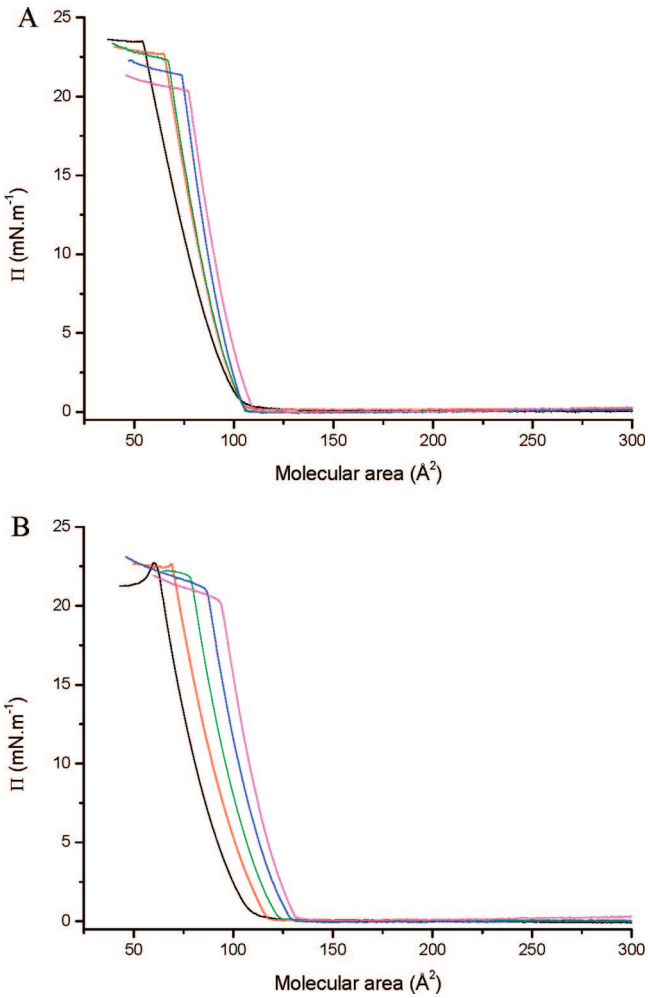

Figure 6. Π−*A* isotherms of the films formed with (A) **CE1** and (B) **CE2** derivatives on the pure water. Temperature: (black line) 20 °C, (red line) 30 °C, (green line) 40 °C, (blue line) 50 °C, (magenta line) 60 °C.

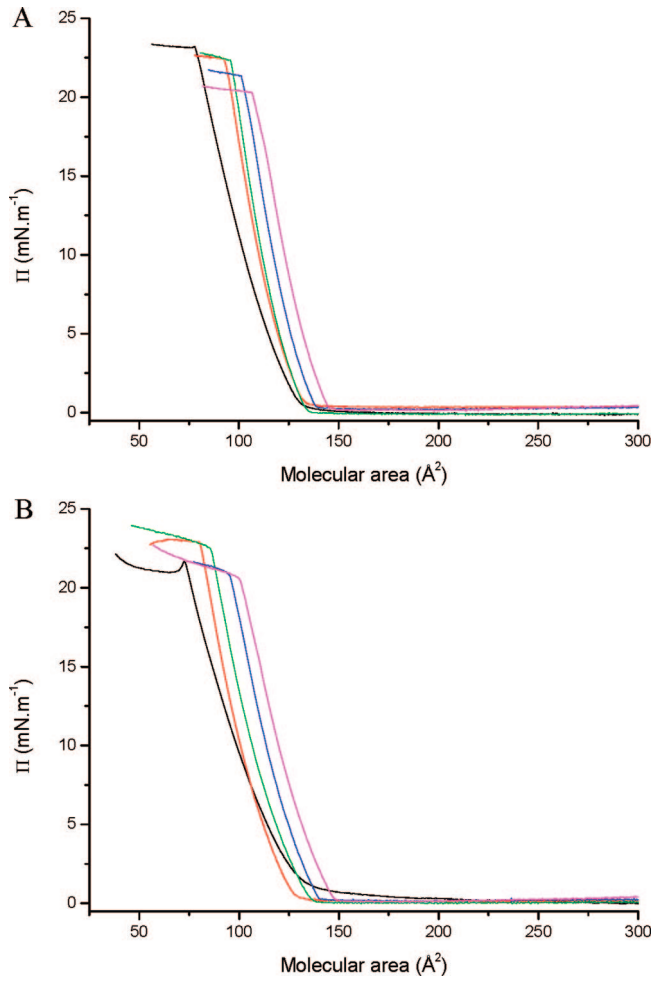

Figure 7. Π−*A* isotherms of the films formed with (A) **CE1** and (B) **CE2** on 10^{-1} M LiCl solution. Temperature: (black line) 20 °C, (red line) 30 °C, (green line) 40 °C, (blue line) 50 °C, (magenta line) 60 °C.

TABLE 3: Characteristic Parameters of the Compression Isotherms Obtained at Different Temperatures on the Pure Water Subphase

temperature [°C]	$C_s^{-1}(A_0)$ [mN m^{-1}]	A_0 [Å^2]	A_{coll} [Å^2]	Π_{coll} [mN m^{-1}]	$C_s^{-1}(A_{coll})$ [mN m^{-1}]
		CE1			
20	57.0	92	54	23.5	33.5
30	71.4	95	65	22.7	48.5
40	76.6	94	67	22.3	54.2
50	89.0	97	74	21.4	67.5
60	86.6	101	77	20.3	66.1
		CE2			
20	67.1	94	60	23.0	43.1
30	70.9	102	69	22.6	48.2
40	81.2	108	79	21.7	59.4
50	87.6	114	87	20.9	66.5
60	92.3	120	94	20.0	72.1

by the positive values of $\Delta\Delta S$ ($\Delta S_{LiCl} - \Delta S_{water}$). Moreover, the C_s^{-1} values decrease with increasing concentration of LiCl in the subphase (Table 1), indicating that the ordering of the **CE2** molecules in the film decreases accordingly, is consistent with the entropy results. In the case of **CE1**, the C_s^{-1} values increase with increasing concentration of LiCl (Table 1) is again consistent with the entropy calculations. The overall results suggest that the conformational changes induced by the complexation of the lithium cation lead to less favorable interactions between the hydrocarbon chains in **CE2** compared to free ligands, while favoring the interactions between the **CE1** molecules; the latter effect would result from the interactions between the crowns. In the future, the advanced solid state and solution NMR studies could be used to help understand better these observations.

On the basis of the compression isotherms (Figure 5, Table 2), it can be supposed that the thermodynamic properties of the monolayers formed with the sodium and potassium complexes of **CE1** and **CE2** are close to those of the lithium complexes. The isotherms obtained with **CE1** and **CE2** in the presence of the di- and trivalent cations show that the corresponding monolayers have different properties compared to the monovalent cations. One can suppose that the complexes formed with di- and trivalent cations would have different conformations compared to the complexes formed with monovalent cations. To get more understanding of the conformational behavior of the two crown ether derivatives upon cation complexation, molecular modeling was performed.

3.2. Modeling. The located structures of **CE1** and its complexes formed with the mono- and divalent cations are shown in Figure 8. The results obtained with **CE2** are close to those obtained with **CE1** and are not shown. Panels (A), (B-G), and (H-M) correspond to the free **CE1** ligand, to its complexes with monovalent ions and to the divalent cation complexes, respectively. Two different coordination modes

TABLE 4: Characteristic Parameters of the Compression Isotherms Obtained at Different Temperatures with 10^{-1} M LiCl Subphase

temperature [°C]	$C_s^{-1}(A_0)$ [mN m^{-1}]	A_0 [Å^2]	A_{coll} [Å^2]	Π_{coll} [mN m^{-1}]	$C_s^{-1}(A_{coll})$ [mN m^{-1}]
		CE1			
20	67.4	119	78	23.2	44.1
30	94.9	122	94	21.8	72.9
40	101.9	123	96	22.0	79.9
50	101.9	129	106	18.2	83.7
60	94.3	138	111	17.7	76.4
		CE2			
20	57.7	117	72	21.7	35.8
30	77.9	114	81	22.7	55.1
40	78.7	120	86	22.4	56.2
50	78.0	130	96	20.5	57.4
60	75.3	138	101	20.4	54.7

TABLE 5: Thermodynamic Parameters* of the Monolayers Formed with the CE1 and CE2 Derivatives on Pure Water and on 10^{-1}M LiCl Solution Subphases

	CE1		**CE2**	
temperature	$\Delta G_{\mathbf{CE1}\ water}$	$\Delta G_{\mathbf{CE1}\ LiCl}$	$\Delta G_{\mathbf{CE2}\ water}$	$\Delta G_{\mathbf{CE2}\ LiCl}$
293.15	9540	12579	10288	11744
303.15	9932	13045	10997	12229
313.15	10493	13653	11879	12867
323.15	10657	13896	12540	13480
333.15	10810	14126	13189	13904

CE1		**CE2**	
$\Delta H_{\mathbf{CE1}\ water}$	$\Delta H_{\mathbf{CE1}\ LiCl}$	$\Delta H_{\mathbf{CE2}\ water}$	$\Delta H_{\mathbf{CE2}\ LiCl}$
63	1100	−11200	−4600

CE1			**CE2**		
$\Delta S_{\mathbf{CE1}\ water}$	$\Delta S_{\mathbf{CE1}\ LiCl}$	$\Delta\Delta S$	$\Delta S_{\mathbf{CE2}\ water}$	$\Delta S_{\mathbf{CE2}\ LiCl}$	$\Delta\Delta S$
−32.7	−39.5	−6.8	−73.5	−55.7	17.8

* Thermodynamic parameter values are given in J mol^{-1}; temperature is in K.

yielding different molecular conformations were found. In the first mode (chair conformation; conformer I), the cation is coordinated by the two crown oxygen atoms (panels B-D and H-J). In the second mode (twisted-boat conformation; conformer II), the cation is located in a cage formed by four atoms, namely two sugar cycle and two ester bond oxygens (panels E-G and K-M).

In Table 6 are listed the interaction energies: $E_{INT} = E_{BA} - E_A - E_B$, where BA, A and B are the complex, the acid (mono- or divalent cation) and the base (crown ether derivative), respectively. All complexes are thermodynamically stable ($E_{INT} < 0$). The stabilization decreases with the increasing ionic/covalent radii (R): $E_{INT}^{CE1\text{-}Li^+} < E_{INT}^{CE1\text{-}Na^+} < E_{INT}^{CE1\text{-}K^+}$ and $E_{INT}^{CE1\text{-}Mg^{2+}} < E_{INT}^{CE1\text{-}Ca^{2+}}$ [$R_{Li^{22}} = 0.76$ Å (1.34 Å), $R_{Na^+} = 1.02$ Å, (1.54 Å), $R_{K^+} = 1.38$ Å (1.96 Å) and $R_{Mg^{2+}} = 0.72$ Å (1.30 Å), $R_{Ca^{2+}} = 0.99$ Å (1.74 Å)]. The highest stabilization is observed with Zn^{2+}. It should be noticed that the ionic/covalent radius of Zn^{2+} [$R_{Zn^{2+}} = 0.74$ Å (1.31 Å)] is close to that of Mg^{2+}. Interestingly, the complexes formed with divalent cations are more stable compared to those formed with monovalent cations. The data collected in Table 6 show that, within the assumed accuracy, there is no stability difference between the **CE1** and **CE2** complexes. This result indicates that the terminal CH_2 groups in the lateral chains have no effect on the bonds formed between the cation and the oxygens; the latter is in agreement with the near-sightedness approximation.[62]

In all cases, conformer II is more stable compared to conformer I. The differences between the conformers are more important with the divalent cations compared to the monovalent cations.

The calculated molecular areas of **CE1** and its complexes are summarized in Table 7. All values were obtained by integrating the contour plot of electron density [$\rho(\vec{r})$]; in other words, the molecular area is enclosed by a $\rho(\vec{r}) < \varepsilon$ contour, where ε is small positive number (10^{-4}). The electron density was computed on a surface perpendicular to the molecular symmetry axis.

It is interesting to notice that, taking into account conformers I and II, the molecular areas of **CE1**−Mg^{2+}, **CE1**−Ca^{2+}, and **CE1**−Zn^{2+} are smaller compared to **CE1**−Li^+, **CE1**−Na^+ and **CE1**−K^+; the latter is in accordance with the experimental results (Figure 5, Table 2). The molecular area of the free **CE1** ligand is between those of the complexes formed with divalent and monovalent cations. The same tendency is observed with **CE2** derivative (results not shown). In agreement with the experimental A_0 values, the smallest molecular area among the systems containing monovalent cations corresponds to **CE1**−K^+. It can be noticed that the difference between the molecular areas of the two conformers is the smallest with the latter cation. The small difference between the interaction energies for these conformers suggests that both of them may exist in an aqueous environment; it cannot be excluded that conformer I is better stabilized in water compared to conformer II (Figure 5, Table 2).

The bond-order (BO) data calculated according to the CBO and CIBO schemes are listed in Tables 8 and 9. The first scheme takes into account only covalent BO (CBO)[63] contributions while the second includes both covalent and ionic BO (CIBO)[64] contributions. It should be noted that, first, the ionic contribution resulting from the interactions between the cation and distributed multipoles change significantly the total valence of the central cation and that, second, several atoms contribute to the total valence of the central atom. The obtained BO values are quite different compared to the typical covalent bond-order data, e.g. C−H, C−C, C−O, and O−H bond orders are close to unity with both CBO and CIBO schemes, since the ionic contribution that differentiates the BO schemes is negligible. The same is valid for the double and triple bonds. Therefore, the total valence of C, N, and O is dominated by contributions from the nearest (chemically bonded) neighbors. The CIBO total valences are always more important for conformer II compared to conformer I. The interaction energies listed in Table 6 show the same tendency. It can be observed that the CBO total valences do not show such a correlation. However, the stronger the covalent contribution (see CBO data), the lower the charge is of the central cation. The data colleted in Table 8 clearly indicate an electrostatic nature of the interactions in all complexes. The central ion preserves its ionic character and the charges are close to the formal oxidation numbers.

4. Conclusions

The monomolecular film experiments showed that two new amphiphilic 1,1′-dioxo-3,3′-dithio-14-crown ether derivatives spread at the air/water interface differentiate between monovalent versus di- or trivalent metal cations present in the aqueous subphase. Molecular modeling supports our proposal that the differentiation observed in compression isotherms is due to the formation of complexes between the crown ether derivatives and the cations. Indeed, modeling showed that the complexes formed with divalent cations are, first, more stable and, second,

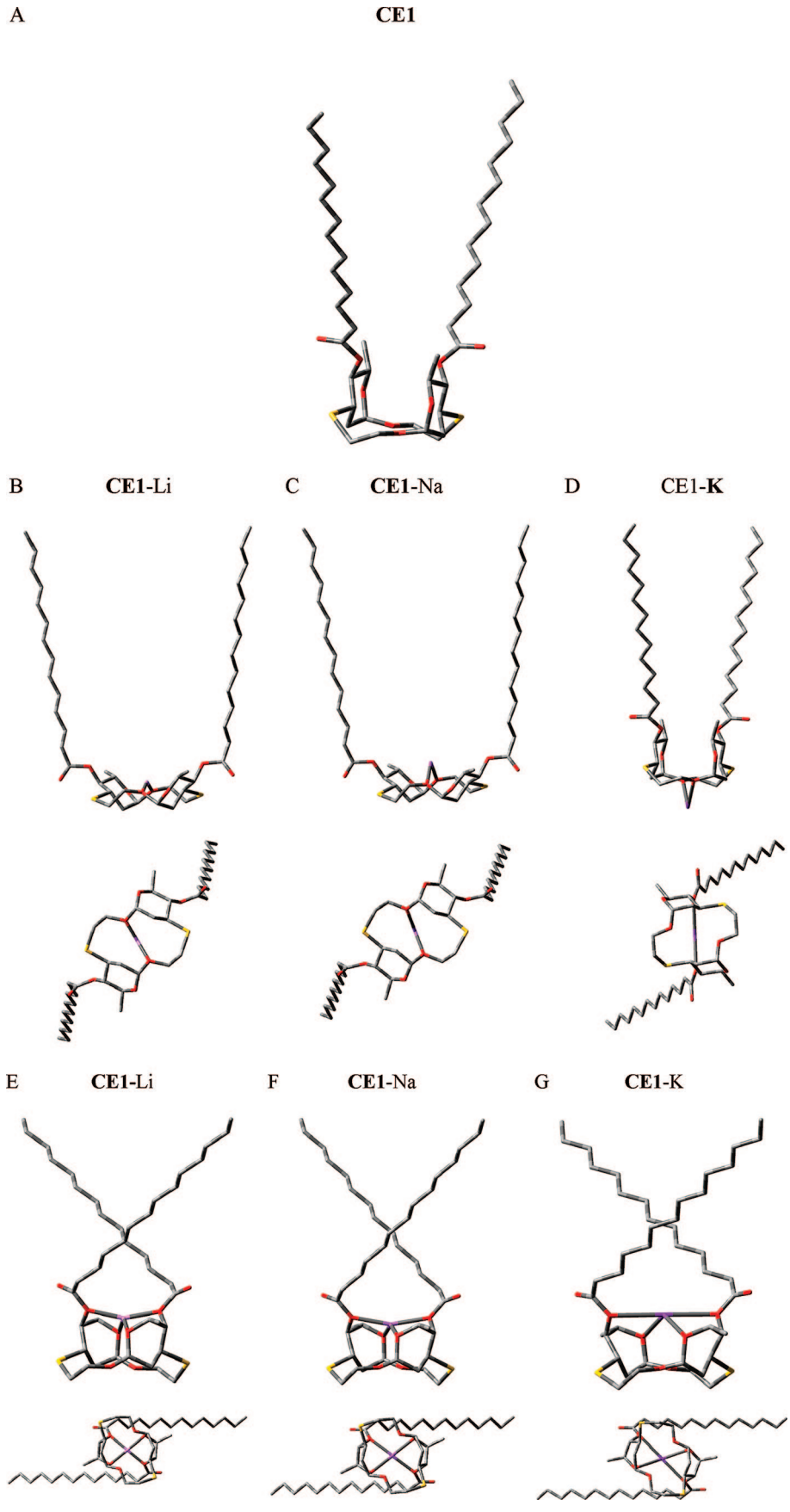

Figure 8

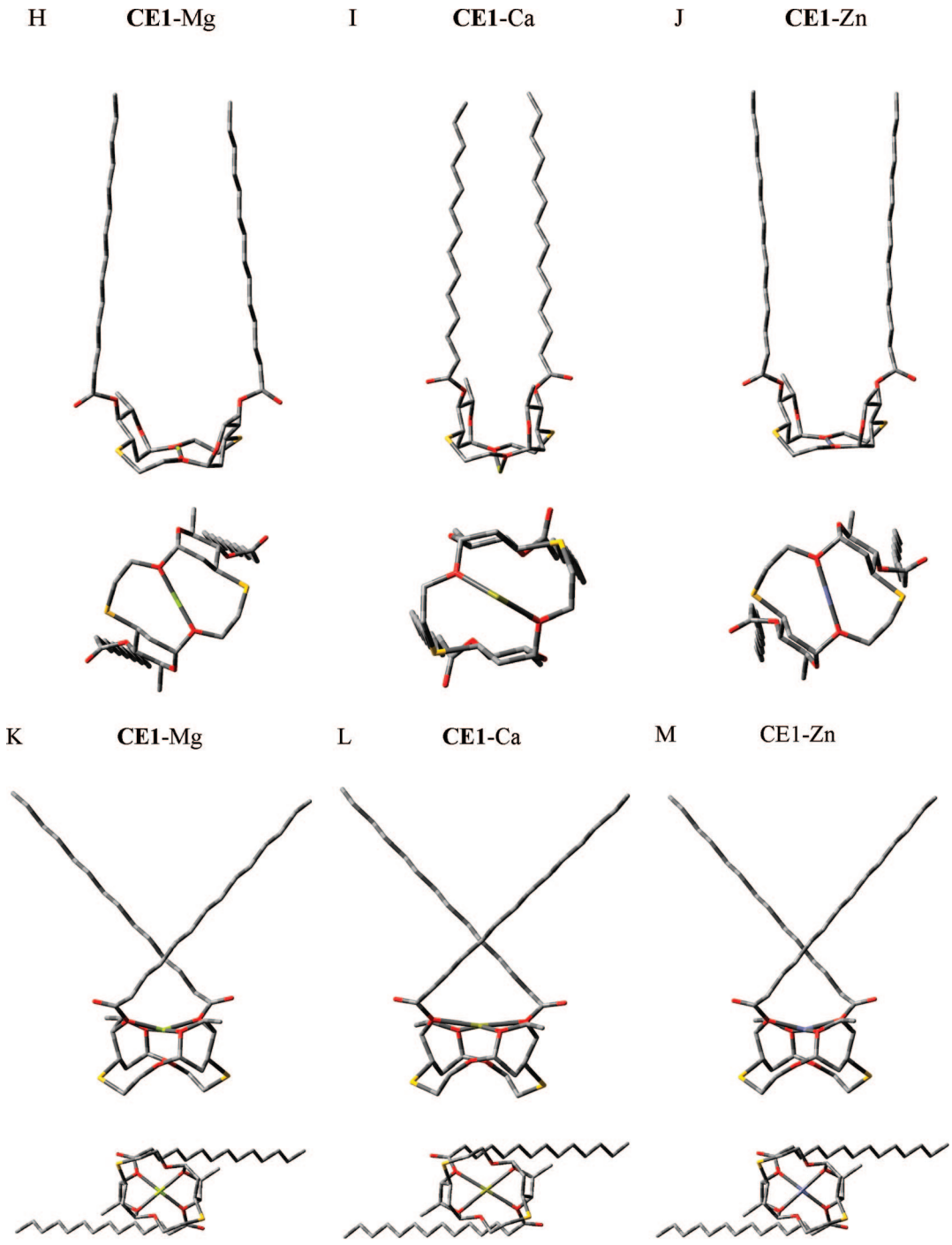

Figure 8. Side and top views of the geometrical structures of the free **CE1** ligand (A) and its complexes with Li^+, Na^+, K^+ (B−G) and Mg^{2+}, Ca^{2+}, Zn^{2+} (H−M). The hydrogens were removed for clarity. Conformer I: panels B−D and H−J. Conformer II: panels E−G and K−M.

adopt conformations yielding smaller molecular areas compared to those formed with monovalent cations; the latter is in accordance with the monolayer experiment results. Thermodynamic calculations demonstrated that, in the presence of lithium cations, the interactions between the crown ether derivatives in the films are repulsive and that more work is needed to form the films compared to pure water; this outcome is in accordance with the monolayer and modeling results showing that the complexes formed with the lithium cation have a more voluminous conformation compared to free ligands. As indicated by the entropy calculations, the more pronounced differentiation between the monovalent and di- or trivalent cations by the

TABLE 6: Interaction Energies ($E_{INT} = E_{AB} - E_A - E_B$) Obtained at the HF Level of Theory with the 6-31G Basis Set for All Located Complexes

	E_{INT} (kcal mol^{-1})			
	conformer I		conformer II	
cation	**CE1**	**CE2**	**CE1**	**CE2**
Li^+	−63.2	−63.3	−65.2	−65.1
Na^+	−34.5	−34.5	−46.0	−46.0
K^+	−19.5	−19.5	−27.4	−27.5
Mg^{2+}	−195.9	−196.0	−247.7	−247.6
Ca^{2+}	−111.4	−111.4	−171.5	−171.5
Zn^{2+}	−222.4	−222.4	−265.3	−265.2

TABLE 7: Calculated Molecular Areas of CE1 and Its Complexes (Å^2) at the HF Level of Theory with a 6-31G Basis Set

	S [Å^2]	
	conformer I	conformer II
CE1	97.1	
CE1−Li^+	129.3	98.7
CE1−Na^+	132.8	99.6
CE1−K^+	105.8	106.0
CE1−Mg^{2+}	105.2	95.2
CE1−Ca^{2+}	87.9	96.4
CE1−Zn^{2+}	91.9	92.6

TABLE 8: Cation−crown Oxygen Bond Orders and Total Valences of Cations for Each Located Conformer I at the RHF/6-31G Level of Theory[a]

conformer I	bond orders	total valences	charges
CE1−Li^+	0.127	0.491	0.75
	0.295	1.483	
CE1−Na^+	0.081	0.304	0.85
	0.203	1.119	
CE1−K^+	0.048	0.371	0.81
	0.103	0.951	
CE1−Mg^{2+}	0.201	0.885	1.53
	0.411	1.885	
CE1−Ca^{2+}	0.086	0.430	1.77
	0.226	1.230	
CE1−Zn^{2+}	0.334	1.165	1.45
	0.551	2.109	

[a] The first and second line in each entry shows CBO and CIBO, respectively. The last column corresponds to Mulliken charges on the central cation.

TABLE 9: Cation−Sugar Ring (Column 2) and Ester Bond (Column 3) Oxygens Bond Orders and Total Valences of Cations for Each Located Conformer II at the RHF/6-31G Level of Theory[a]

conformer II	bond-orders		total valences	charges
CE1−Li^+	0.128	0.111	0.618	0.68
	0.176	0.221	1.645	
CE1−Na^+	0.096	0.076	0.611	0.69
	0.159	0.159	1.511	
CE1−K^+	0.062	0.048	0.519	0.74
	0.076	0.069	1.190	
CE1−Mg^{2+}	0.161	0.127	0.689	1.63
	0.261	0.256	1.953	
CE1−Ca^{2+}	0.096	0.076	0.676	1.65
	0.156	0.152	1.720	
CE1−Zn^{2+}	0.210	0.177	0.920	1.58
	0.319	0.304	2.123	

[a] The first and second line in each entry shows CBO and CIBO, respectively. The last column corresponds to Mulliken charges on the central cation.

derivative bearing the shorter hydrocarbon chains may be due to its lower ordering in the film.

The cation differentiation observed with the two crown ether derivatives may be interesting in the further studies on their potential ionophore activity. Indeed, it was shown recently that the antimalarial activity of carboxylic polyether antibiotics is linked to the selectivity for monovalent versus divalent cations, but not the selectivity for Na^+ versus K^+.[65,66] On the other hand, the results obtained show that the length of the hydrocarbon chains is decisive for the interfacial properties of the crown ether derivatives; it may be important for the perturbation of the lipid membrane structure[67] and for such effects as the transport rate.

Acknowledgment. The Ministère de la Recherche et de l'Enseignement Supérieur and the Centre National de la Recherche Scientifique are acknowledged for their financial support. B.K. acknowledges a 3 months fellowship from Université Henri Poincaré Nancy 1. We thank Dr. Matthew Fielden (KSV, Finland) for proof-reading the manuscript. The work carried out by J.K. was supported by The Polish Ministry of Science and Higher Education (Project No. 1206/GDR/2007/03). The Computational Grants MNiSW/SGI3700/UJ/161/2006 and MEiN/SGI3700/UJ/108/2006 are greatly acknowledged.

References and Notes

(1) Pedersen, C. J. *J. Am. Chem. Soc.* **1967**, *89*, 2495–2496.
(2) Pedersen, C. J. *J. Am. Chem. Soc.* **1967**, *89*, 7017–7036.
(3) Gokel, G. W.; Leevy, W. M.; Weber, M. E. *Chem. Rev.* **2004**, *104*, 2723–2750.
(4) Sannicolo, F.; Brenna, E.; Benincori, T.; Zotti, G.; Zecchin, S.; Schiavon, G.; Pilati, T. *Chem. Mater.* **1998**, *10*, 2167–2176.
(5) Tokunaga, Y.; Nakamura, T.; Yoshioka, M.; Shimomura, Y. *Tetrahedron Lett.* **2006**, *47*, 5901–5904.
(6) Mathias, L. J. *J. Macromol. Sci., Chem.* **1981**, *A15*, 853–876.
(7) Tran, C. D.; Zhang, W. *Anal. Chem.* **1990**, *62*, 830–834.
(8) Chen, S.; Yuan, H.; Grinberg, N.; Dovletoglou, A.; Bicker, G. *J. Liq. Chromatogr. Relat. Technol.* **2003**, *26*, 425–442.
(9) Kuwahara, Y.; Nagata, H.; Nishi, H.; Tanaka, Y.; Kakehi, K. *Chromatographia* **2005**, *62*, 505–510.
(10) Munoz, S.; Mallen, J.; Nakano, A.; Chen, Z.; Gay, I.; Echegoyen, L.; Gokel, G. W. *J. Am. Chem. Soc.* **1993**, *115*, 1705–1711.
(11) Mazik, M.; Kuschel, M.; Sicking, W. *Org. Lett.* **2006**, *8*, 855–858.
(12) Cazacu, A.; Tong, C.; Van der Lee, A.; Fyles, T. M.; Barboiu, M. *J. Am. Chem. Soc.* **2006**, *128*, 9541–9548.
(13) Inoue, Y., Gokel, G. W. Eds. *Cation Binding by Macrocycles*; Marcel Dekker: New York, 1990.
(14) Gokel, G. W. Crown Ethers and Cryptands. In *Monographs in Supramolecular Chemistry*; Stoddart, J. F., Ed.; The Royal Society of Chemistry: Cambridge, England, 1991.
(15) Izatt, R. M.; Bradshaw, J. S.; Nielsen, S. A.; Lamb, J. D.; Christensen, J. J.; Sen, D. *Chem. Rev.* **1985**, *85*, 271–339.
(16) Izatt, R. M.; Pawlak, K.; Bradshaw, J. S.; Bruening, R. L. *Chem. Rev.* **1991**, *91*, 1721–1785.
(17) Gokel, G. W.; Goli, D. M.; Minganti, C.; Echegoyen, L. *J. Am. Chem. Soc.* **1983**, *105*, 6786–6788.
(18) de Wall, S. L.; Wang, K.; Berger, D. R.; Watanabe, S.; Hernandez, J. C.; Gokel, G. W. *J. Org. Chem.* **1997**, *62*, 6784–6791.
(19) Tsukube, H.; Hamada, T.; Tanaka, T.; Uenishi, J. *Inorg. Chim. Acta* **1993**, *214*, 1–3.
(20) Furusawa, K.; Obata, C.; Matsumura, H.; Takeuchi, M.; Kuwamura, T. *Chem. Lett.* **1990**, 1047–1050.
(21) Okahara, M.; Kuo, P.-L.; Yamamura, S.; Ikeda, I. *J. Chem. Soc., Chem. Commun.* **1980**, 586–587.
(22) Fernandez-Lazaro, F.; Sastre, A.; Torres, T. *J. Chem. Soc., Chem. Commun.* **1995**, 419–420.
(23) Ozeki, S.; Kojima, A.; Harada, S.; Inokuma, S.; Takahashi, H.; Kuwamura, T.; Uchiyama, H.; Abe, M.; Ogino, K. *J. Phys. Chem.* **1990**, *94*, 8207–8212.
(24) Ozeki, S.; Harada, S.; Kojima, A.; Abe, M.; Ogino, K.; Takahashi, H.; Inokuma, S.; Kuwamura, T. *J. Phys. Chem.* **1990**, *94*, 8213–8217.
(25) Wojciechowski, K.; Grigoriev, D.; Ferdani, R.; Gokel, G. W. *Langmuir* **2006**, *22*, 8409–8415.
(26) Badis, M.; Tomaszkiewicz, I.; Joly, J.-P.; Rogalska, E. *Langmuir* **2004**, *20*, 6259–6267.
(27) Zawisza, I.; Bilewicz, R.; Luboch, E.; Biernat, J. F. *Dalton* **2000**, 499–503.
(28) Lednev, I. K.; Petty, M. C. *Adv. Mater.* **1996**, *8*, 615–630.
(29) Plehnert, R.; Schroeter, J. A.; Tschierske, C. *Langmuir* **1998**, *14*, 5245–5249.
(30) Shahgaldian, P.; Pieles, U.; Hegner, M. *Langmuir* **2005**, *21*, 6503–6507.
(31) Sergeeva, T. I.; Zaitsev, S. Y.; Tsarkova, M. S.; Gromov, S. P.; Vedernikov, A. I.; Kapichnikova, M. S.; Alfimov, M. V.; Druzhinina, T. S.; Mobius, D. *J. Colloid Interface Sci.* **2003**, *265*, 77–82.
(32) Zaitsev, S. Y.; Sergeeva, T. I.; Baryshnikova, E. A.; Gromov, S. P.; Fedorova, O. A.; Alfimov, M. V.; Hacke, S.; Mobius, D. *Colloids Surf. A* **2002**, *198−200*, 473–482.
(33) Muszalska, E.; Bilewicz, R.; Luboch, E.; Skwierawska, A.; Biernat, J. F. *J. Inclusion Phenom.* **1996**, *26*, 47–59.
(34) Korchowiec, B.; Ben Salem, A.; Corvis, Y.; Regnouf de Vains, J.-B.; Korchowiec, J.; Rogalska, E. *J. Phys. Chem. B* **2007**, *111*, 13231–13242.

(35) Lu, G.; Tang, N.; Sun, Y.; Wang, H. *Synth. Commun.* **2006**, *36*, 3829–3836.
(36) Doyle, D. A.; Cabral, J. M.; Pfuetzner, R. A.; Kuo, A.; Gulbis, J. M.; Cohen, S. L.; Chait, B. T.; MacKinnon, R. *Science* **1998**, *280*, 69–77.
(37) Zhou, Y.; Morais-Cabral, J. H.; Kaufman, A.; MacKinnon, R. *Nature* **2001**, *414*, 43–48.
(38) Dutzler, R.; Campbell, E. B.; Cadene, M.; Chait, B. T.; MacKinnon, R. *Nature* **2002**, *415*, 287–294.
(39) Jiang, Y.; Lee, A.; Chen, J.; Ruta, V.; Cadene, M.; Chait, B. T.; MacKinnon, R. *Nature* **2003**, *423*, 33–41.
(40) Gokel, G. W. *Chem. Commun.* **2000**, 1–9.
(41) Murillo, O.; Watanabe, S.; Nakano, A.; Gokel, G. W. *J. Am. Chem. Soc.* **1995**, *117*, 7665–7679.
(42) Murillo, O.; Suzuki, I.; Abel, E.; Murray, C. L.; Meadows, E. S.; Jin, T.; Gokel, G. W. *J. Am. Chem. Soc.* **1997**, *119*, 5540–5549.
(43) Abel, E.; Meadows, E. S.; Suzuki, I.; Jin, T.; Gokel, G. W. *Chem. Commun.* **1997**, 1145–1146.
(44) Leevy, W. M.; Donato, G. M.; Ferdani, R.; Goldman, W. E.; Schlesinger, P. H.; Gokel, G. W. *J. Am. Chem. Soc.* **2002**, *124*, 9022–9023.
(45) Agre, P.; Kozono, D. *FEBS Lett.* **2003**, *555*, 72–78.
(46) Pohl, P. *Biol. Chem.* **2004**, *385*, 921–926.
(47) Mannuzzu, L. M.; Moronne, M. M.; Isacoff, E. Y. *Science* **1996**, *271*, 213–216.
(48) Munson, K.; Law, R. J.; Sachs, G. *Biochemistry* **2007**, *46*, 5398–5417.
(49) Siu, S. W. I.; Boeckmann, R. A. *J. Struct. Biol.* **2007**, *157*, 545–556.
(50) Sands, Z. A.; Sansom, M. S. P. *Structure* **2007**, *15*, 235–244.
(51) Cohen, E.; Goldshleger, R.; Shainskaya, A.; Tal, D. M.; Ebel, C.; le Maire, M.; Karlish, S. J. D. *J. Biol. Chem.* **2005**, *280*, 16610–16618.
(52) Wallace, B. A. *J. Struct. Biol.* **1998**, *121*, 123–141.
(53) Ditchfield, R.; Hehre, W. J.; Pople, J. A. *J. Chem. Phys.* **1971**, *54*, 724–728.
(54) Hehre, W. J.; Ditchfield, R.; Pople, J. A. *J. Chem. Phys.* **1972**, *56*, 2257–2261.
(55) GAMESS/Version 14, Jan. 2003 (R2) from Iowa State University.
(56) Schmidt, M. W.; Baldridge, K. K.; Boatz, J. A.; Elbert, S. T.; Gordon, M. S.; Jensen, J. H.; Koseki, S.; Matsunaga, N.; Nguyen, K. A.; et al. *J. Comput. Chem.* **1993**, *14*, 1347–1363.
(57) *Gaussian 03, Revision D.01*, Gaussian, Inc.: Wallingford, CT, 2004.
(58) Davies, J. T.; Rideal, E. K. *Interfacial Phenomena*, 2nd ed.; 1963.
(59) Korchowiec, B.; Paluch, M.; Corvis, Y.; Rogalska, E. *Chem. Phys. Lipids* **2006**, *144*, 127–136.
(60) Sorai, M.; Saito, K. *Chem. Rec.* **2003**, *3*, 29–39.
(61) Stachowiak, C.; Viguie, J.-R.; Grolier, J.-P. E.; Rogalski, M. *Langmuir* **2005**, *21*, 4824–4829.
(62) Kohn, W. *Phys. Rev. Lett.* **1996**, *76*, 3168–3171.
(63) Nalewajski, R. F.; Mrozek, J. *Int. J. Quantum Chem.* **1994**, *51*, 187–200.
(64) Mayer, I. *Theor. Chim. Acta* **1985**, *67*, 315–322.
(65) Gibot, S.; Jeminet, G.; Juillard, J.; Gumila, C.; Ancelin, M.-L.; Vial, H.; Delort, A.-M. *Arch. Biochem. Biophys.* **1999**, *363*, 361–372.
(66) Gumila, C.; Ancelin, M.-L.; Delort, A.-M.; Jeminet, G.; Vial, H. J. *Antimicrob. Agents Chemother.* **1997**, *41*, 523–529.
(67) Gumila, C.; Miquel, G.; Seta, P.; Ancelin, M.-L.; Delort, A.-M.; Jeminet, G.; Vial, H. J. *J. Colloid Interface Sci.* **1999**, *218*, 377–387.

JP803072B